Performance and Complexity Comparison of MRC and PASTd-based Statistical Beamforming and Eigencombining

Constantin Siriteanu, Xin Guan, Steven D. Blostein

***Abstract*—Smart antennas may enhance performance by applying conventional algorithms such as maximal-ratio combining (MRC) or maximum average signal-to-noise-ratio beamforming, i.e., statistical beamforming (BF). However, MRC and BF yield advantages that offset their complexity only for extreme antenna correlation values, which seldom occur for space-limited base-station antenna arrays deployed in typical urban (TU) scenarios, with predominantly-small, random, azimuth spread (AS). Therefore, the principles of BF and MRC have been integrated to forge maximal-ratio eigencombining (MREC), which promises to reap the available array and diversity gains more effectively. Nonetheless, the relative performance and numerical complexity of MREC, BF, and MRC have not yet been investigated for channel estimated from received-signal-vector samples in a TU uplink scenario with realistic Laplacian base-station power azimuth spectrum and log-normally distributed AS with exponential temporal correlation. Therefore, herein, Yang's effective and low-complexity deflation-based projection approximation subspace tracking (PASTd) algorithm is deployed to recursively update the channel eigenstructure required for MREC adapted to AS using the classical bias-variance tradeoff criterion (BVTC). Simulation results indicate that BVTC-based MREC can significantly outperform BF for much lower complexity than MRC.**

***Index Terms*—Azimuth spread, fading estimation, maximal-ratio eigen-combining, projection approximation subspace tracking.**

I. INTRODUCTION

Wireless communications standards (3GPP/2, WiMAX, WiFi, etc.) specify smart antenna algorithms [1] designed to take advantage of array and diversity gains [2, Sections 5.2, 5.3]. For receive antennas, full array gain is only achievable with coherent combining. Then, full diversity gain is only achievable for uncorrelated fading channel gains. However, actual received-power azimuth spread (AS) values [3] and channel fading estimation errors [4, Section 3.6] can seriously degrade the performance of classical combining techniques such as maximal-ratio combining (MRC) [5] [6], and maximum average signal-to-noise ratio (SNR) beamforming, i.e., statistical beamforming (BF) [6] [7].

BF combines the received signal vector with a vector parallel to the dominant eigenvector of the channel correlation matrix. Thus, BF performance degrades due to combiner–channel coherence loss in non-zero AS [5] [6] [7]. On the other hand, MRC combines the received signal vector with the channel gain vector, which is in practice estimated through numerically complex operations [4] [5] [8]. Furthermore, MRC performs best for uncorrelated channel gains [4] [5] [6]. However, in typical urban (TU) scenarios the base station 'sees' a Laplacian power azimuth spectrum (p.a.s.) with a predominantly small-to-moderate AS that fluctuates randomly, orders of magnitude slower than the Doppler-shift-induced fading [4] [5]. Therefore, BF and MRC may periodically underperform or have oversized numerical complexity [5] [8].

Maximal-ratio eigencombining (MREC) [5] [6] [9] consists of projecting the received signal vector onto dominant eigenvectors of the channel gain correlation matrix — i.e., the Karhunen-Loeve Transform (KLT) — followed by MRC. Therefore, MREC is a superset of BF and MRC [4, Section 3.9] [5] that has been promoted as able to extract the available array and diversity gains for lower complexity than MRC, and to simplify performance analysis [4] [5] [7] [9] [10].

MREC, MRC, and BF performance and complexity have been compared for the unrealistic assumption of perfectly known channel eigenstructure (eigenvectors and eigenvalues) in [4] [5] [6] [8] [9] [10]. Representative eigenstructure tracking methods are summarized in [11] [12]. The novel method introduced in [12] and applied for eigencombining in [7, Section 4.3] is more complex than Yang's projection approximation subspace tracking with deflation (PASTd) [11], which, nevertheless, converges fast to good approximations of the eigenstructure, and is robust with respect to input signal conditioning. Furthermore, [7] used a stochastic channel model that requires tracking the relative positions of the mobile stations with respect to many stationary scatterers and the base station, and thus can lead to long simulations, unlike the realistic AS-based 3GPP channel model [13]. Finally, [7] did not optimize eigenvector, i.e., MREC-order, selection. In [5] we proposed MREC adaptation using a bias-variance tradeoff criterion (BVTC), but evaluated the symbol-detection performance only based on mathematical analysis (as opposed to simulation), and only for perfectly known channel eigenstructure.

Realistic MREC, MRC, and BF performance and complexity comparisons are presented herein based on simulations for: 1) the 3GPP spatial channel model [13] for base-station receive antenna arrays in TU scenarios, i.e., with realistic Laplacian p.a.s. of log-normally distributed AS; additionally, the tempo-

C. Siriteanu (email: costi@cse.snu.ac.kr) is a "Brain Korea 21st Century" Assistant Professor with the School of Computer Science and Engineering, Seoul National University, Korea.

X. Guan (email: guanxinstephen@hotmail.com) is a Master's student in the Digital Communications Laboratory at Hanyang University. His work has been supported by the "Brain Korea 21st Century" and the "LG Global Track" programs.

S. D. Blostein (steven.blostein@queensu.ca) is with the Department of Electrical and Computer Engineering, Queen's University, Kingston, Canada.

ral correlation of the AS is modeled as exponential [3, Eqn. (14)]; 2) low-complexity PASTd-based channel eigenstructure estimation using samples of the received signal vector; 3) MREC order selected adaptively using the BVTC; 4) optimum and suboptimum fading estimation [4, Section 3.6] [8, Section 2.6].

The paper is organized as follows. Section II presents the transmitted signal, channel fading, receiver noise, p.a.s., and AS models. Section III describes MREC and its relationships with MRC and BF, as well as channel fading and eigenstructure estimation methods, along with their numerical complexities. Section IV shows simulation results for the performance and complexity of BF, MRC, and adaptive MREC.

II. Signal, Channel, and Noise Models

A. Received Signal Model

A mobile station transmits signal through a frequency-flat Rayleigh fading channel. At an L-element base-station antenna array the received signal vector after demodulation, matched-filtering, and symbol-rate sampling can be written as [5]

$$\widetilde{\mathbf{y}} = \sqrt{E_\mathrm{s}}\, b\, \widetilde{\mathbf{h}} + \widetilde{\mathbf{n}} \tag{1}$$

where b is the equiprobable transmitted symbol, and E_s is the energy transmitted per symbol. For the numerical results shown later we assumed an M–PSK transmitted signal, where M is the constellation size. The channel fading and receiver noise $\widetilde{\mathbf{h}}$ and $\widetilde{\mathbf{n}}$ are assumed to be mutually uncorrelated zero-mean circularly-symmetric complex Gaussian [2, p. 39] random vectors. The noise vector is assumed to be temporally and spatially white with per-element variance equal to N_0, i.e., $\widetilde{\mathbf{n}} \sim \mathcal{N}_c(\mathbf{0}, N_0\mathbf{I})$. The distribution of the channel gain vector

$$\widetilde{\mathbf{h}} \sim \mathcal{N}_c(\mathbf{0}, \mathbf{R}_{\widetilde{\mathbf{h}}}) \tag{2}$$

is completely described by its Hermitian correlation matrix

$$\mathbf{R}_{\widetilde{\mathbf{h}}} \stackrel{\triangle}{=} E\{\widetilde{\mathbf{h}}\widetilde{\mathbf{h}}^H\}. \tag{3}$$

Its eigenvalues are real-valued and non-negative, and are hereafter considered ordered as $\lambda_1 \geq \lambda_2 \geq \ldots \geq \lambda_L \geq 0$. The corresponding, orthonormal, eigenvectors are denoted as $\mathbf{u}_i$, $i = 1:L$. The eigendecomposition of $\mathbf{R}_{\widetilde{\mathbf{h}}}$ is then described by

$$\mathbf{R}_{\widetilde{\mathbf{h}}} = \mathbf{U}_L \mathbf{\Lambda}_L \mathbf{U}_L^H = \sum_{i=1}^{L} \lambda_i \mathbf{u}_i \mathbf{u}_i^H, \tag{4}$$

where $\mathbf{\Lambda}_L$ and $\mathbf{U}_L$ are a diagonal and a unitary matrix formed with the eigenvalues and eigenvectors of $\mathbf{R}_{\widetilde{\mathbf{h}}}$, respectively. Hereafter, the term *dominant eigenvectors* refers to the set of eigenvectors corresponding to the dominant eigenvalues, i.e., those eigenvalues which contribute most to the trace of $\mathbf{R}_{\widetilde{\mathbf{h}}}$.

B. P.A.S. and AS Models

In typical urban (TU) environments the received signal power appears dispersed in azimuth angle following a Laplacian distribution [13] [3]. The Laplacian power azimuth spectrum (p.a.s.) is described by [13, Section 4.5.4] [6, Eqns. 14, 15] [4, p. 136] as a function of the mean angle of arrival and of the azimuth spread (AS), which is (approximately) the root second central moment of the p.a.s. The correlation between two antenna elements can then be computed using the expressions [6, Eqn. 16] [4, Eqns. (4.3)-(4.4), pp. 136-137].

For the numerical results shown later the 'TU-32' scenario described in [3, Table I] has been considered. Then, the base-station AS, measured in degrees, is well modeled as a lognormally-distributed random variable [3, Eqn. (9)]

$$\mathrm{AS} = 10^{\varepsilon x + \mu}; \quad x \sim \mathcal{N}(0,1), \tag{5}$$

with $\varepsilon = 0.47$ and $\mu = 0.74$ [3, Table II]. Random AS samples then yield $\Pr(1^\circ < \mathrm{AS} < 20^\circ) \approx 0.8$ [5], which implies preponderantly-high (over 0.5) antenna correlation values for compact antenna arrays (with unitary normalized inter-element distance, $d_\mathrm{n} = 1$, i.e., physical distance equals half of the carrier wavelength) [5, Fig. 1].

Finally, the received signal experiences AS fluctuation described by the following correlation expression [3, Eqn. (14)]:

$$\rho_\mathrm{AS}(d) = e^{-d/d_\mathrm{AS}}. \tag{6}$$

Above, d is the mobile displacement and $d_\mathrm{AS} = 70$ m [3, Fig. 4] is the AS *decorrelation distance*.

III. MREC, MRC, and BF

A. MREC Description

We summarize below from [5, Section III.A.1] the steps of maximal-ratio eigencombining (MREC) of order $N = 1:L$, denoted hereafter as MREC_N:

(1) The $L \times N$, full-column rank, matrix $\mathbf{U}_N \stackrel{\triangle}{=} [\mathbf{u}_1\, \mathbf{u}_2\, \ldots\, \mathbf{u}_N]$ transforms the signal vector from (1) into

$$\mathbf{y} = \sqrt{E_\mathrm{s}}\, b\, \mathbf{h} + \mathbf{n}, \tag{7}$$

where

$$\mathbf{y} \stackrel{\triangle}{=} \mathbf{U}_N^H\, \widetilde{\mathbf{y}}, \quad \mathbf{h} \stackrel{\triangle}{=} \mathbf{U}_N^H\, \widetilde{\mathbf{h}}, \quad \mathbf{n} \stackrel{\triangle}{=} \mathbf{U}_N^H\, \widetilde{\mathbf{n}}. \tag{8}$$

This is the well-known Karhunen-Loeve Transform (KLT) [11]. The elements of the N-dimensional vectors $\mathbf{y}$ and $\mathbf{h}$ are hereafter referred to as *eigenbranches* and *eigengains*, respectively. Our assumptions about the fading and noise imply that $\mathbf{h} \sim \mathcal{N}_c(\mathbf{0}, \mathbf{\Lambda}_N)$, i.e., the eigengains are independent, and that $\mathbf{n} \sim \mathcal{N}_c(\mathbf{0}, N_0\mathbf{I}_N)$.

(2) The transformed signal vector is linearly combined based on the maximal-ratio combining criterion [14], with

$$\mathbf{w}_\mathrm{MREC} = \mathbf{h}. \tag{9}$$

Note that $\mathrm{MREC}_{N=1}$ represents the conventional maximal average (over fading and noise) SNR, i.e., statistical, beamforming (BF) technique. BF is typically adopted in scenarios with high inter-branch correlation, to take advantage of array gain [2, Section 5.3]. On the other hand, by skipping Step 1, MREC reduces to the conventional maximal-ratio combining (MRC) technique [14]. MRC is typically adopted to yield diversity gain [2, Section 5.2] for uncorrelated branches. Since, as mentioned in Section II-B, interbranch correlation for compact antennas is predominantly over 0.5 but not always near 1, $\mathrm{MREC}_{N>1}$ was recently suggested [4] [5] to cover the middle ground more effectively.

TABLE I
PASTD ALGORITHM

Operation	Complexity
Initialization:	
$\lambda_{\widetilde{\mathbf{y}},i}(0)=1$, $\mathbf{u}_i(0)=\mathbf{e}_i$, $i=1:N$	
$\mathbf{e}_i$ - ith column of the identity matrix	
FOR $n=1,2,\ldots$ DO % time loop	
$\mathbf{x}_1(n)=\sqrt{1-\beta}\,\widetilde{\mathbf{y}}(n)$	
FOR $i=1,2,\ldots,N$ DO % eigenspace loop	
$\upsilon_i(n)=\mathbf{u}_i^H(n-1)\,\mathbf{x}_i(n)$	L
$\lambda_{\widetilde{\mathbf{y}},i}(n)=\beta\lambda_{\widetilde{\mathbf{y}},i}(n-1)+\lvert\upsilon_i(n)\rvert^2$	
$\lambda_i(n)=(\lambda_{\widetilde{\mathbf{y}},i}(n)-N_0)/E_S$	
$\boldsymbol{\varepsilon}_i(n)=\mathbf{x}_i(n)-\mathbf{u}_i(n-1)\,\upsilon_i(n)$	L
$\mathbf{u}_i(n)=\mathbf{u}_i(n-1)+\boldsymbol{\varepsilon}_i(n)[\upsilon_i^*/\lambda_{\widetilde{\mathbf{y}},i}(n)]$	L
$\mathbf{x}_{i+1}(n)=\mathbf{x}_i(n)-\mathbf{u}_i(n)\,\upsilon_i(n)$	L

B. Channel Estimation

Stand-alone MRC does not require channel eigenstructure knowledge, but requires estimation of the L channel fading gains. On the other hand, MREC requires estimates of the N channel eigengains and the associated eigenstructure. BF requires a single channel eigengain and eigenvector. The eigen/gains vary at the Doppler rate, i.e., much faster than the rate of AS (i.e., eigenstructure) variation [5, p. 918]. Consequently, symbol- and channel-rate signal processing tasks (signal combining, KLT, fading estimation) consume large amounts of baseband processing resources (chip area and power) — see [4, Chapter 5] [8] and references therein. As we shall see, PASTd-based eigendecomposition is much less demanding computationally.

1) PASTd-based Channel Eigenstructure Estimation: Previous MREC studies assumed perfect knowledge of the eigenstructure of $\mathbf{R}_{\widetilde{\mathbf{h}}}$ [4] [5]. In [7] eigencombining performance was evaluated for the high-complexity subspace tracking algorithms proposed in [12]. To demonstrate the complexity-reduction capabilities of MREC over MRC, we will employ Yang's low-complexity deflation-based projection approximation subspace tracking (PASTd) algorithm [11].

Since (7) implies that $\mathbf{R}_{\widetilde{\mathbf{y}}}=E_S\,\mathbf{R}_{\widetilde{\mathbf{h}}}+N_0\,\mathbf{I}$, the eigenvectors of $\mathbf{R}_{\widetilde{\mathbf{h}}}$ and $\mathbf{R}_{\widetilde{\mathbf{y}}}$ coincide, and the ith eigenvalue of $\mathbf{R}_{\widetilde{\mathbf{y}}}$ is $\lambda_{\widetilde{\mathbf{y}},i}=E_S\,\lambda_i+N_0$. Assuming exponentially-weighted sample correlation matrix virtual updating as in [7, Eqn. (13)]

$$\mathbf{R}_{\widetilde{\mathbf{y}}}(n)=\beta\cdot\mathbf{R}_{\widetilde{\mathbf{y}}}(n-1)+(1-\beta)\widetilde{\mathbf{y}}(n)\,\widetilde{\mathbf{y}}(n)^H \tag{10}$$

using temporally-uncorrelated samples of the received signal vector, $\widetilde{\mathbf{y}}(n)$, the PASTd algorithm sequentially updates the N required eigenvectors and eigenvalues as shown in Table I, for per-update numerical complexity (number of multiplications/additions with complex numbers) of about $4LN$. Denoting with K the number of symbols between the samples used for the update in (10), the per-symbol numerical complexity incurred in MREC_N by PASTd is $4LN/K$. The value of K is lower-bounded by the maximum normalized Doppler shift [5, Table I], because the signal samples used in (10) have to be temporally uncorrelated, and is upper-bounded by the AS decorrelation distance — see (6) — assuming that no other factors determine antenna correlation fluctuations.

2) Eigen/Gain Estimation: When the transmitter employs pilot-symbol-aided modulation (PSAM) the channel eigen/gains can be estimated at the receiver by pilot-sample interpolation. In [8, Section 2.6] [4, Section 3.6] [15, Section III.B] two PSAM-based channel estimation methods have been proposed: 1) a data-independent suboptimal interpolation method entitled SINC PSAM (because the time-response of the interpolation filter approaches a sinc function); 2) a data-dependent optimal, interpolation method entitled MMSE PSAM (from minimum mean-squared-error).

These estimation methods are characterized by the PSAM slot length M_S (a slot consists of one pilot symbol followed by M_S-1 data symbols) and by the interpolator size T (the number of pilot samples employed for estimation). SINC and MMSE PSAM have been used for the numerical results shown later. For the numerical results presented later we have assumed a maximum normalized Doppler shift of $f_m=0.01$ (i.e., the symbols arrive at a rate 100 higher than the channel fading rate). Then, appropriate values are $M_S=7$ and $T=11$ [4, p. 36].

3) Comments: For $N=1$, MREC reduces to the classical statistical beamforming (BF) approach [7]. On the other hand, $\text{MREC}_{N=L}$ (*full MREC*) using the actual channel eigenstructure is performance-equivalent with MRC of the original branches if the same linear method is employed to estimate the eigen/gains [4, Section 3.9] [5]. For PASTd-based eigenstructure estimation we shall see that full MREC can still yield near-MRC performance.

Using the estimate of the channel eigen/gain vector as a weight vector for MRC or MREC is not optimal when knowledge about the channel and noise statistics is available. Therefore, this approach has been denoted as 'approximate' eigen/combining [4] [5]. The optimum ('exact') combining approach is described for MRC in [4, Appendix A] and for MREC in [5, Section III.D.1]. For perfectly known channel eigenstructure, average symbol error probability expressions for approximate and exact MREC (thus also for MRC) appear in [4] [5].

C. BF, MRC, and MREC Numerical Complexity Comparison

For SINC PSAM a vector is estimated one component at a time, using inner products [4, Eqn. (3.110), p. 83] [15, Eqn. (42)] [8, Eqn. (4)]. Therefore, the SINC PSAM channel gain estimation for MRC and the SINC PSAM eigengain estimation for MREC have the same complexity. Nonetheless, unlike MRC, MREC requires eigenstructure updating every K symbols and KLT at each symbol. Based on the discussion from Section III-B1 and [5, Table II], the per-symbol numerical complexities involved by the PASTd-based eigenstructure estimation and KLT (for MREC), fading gain/eigengain estimation, and weight–signal combining are shown in Table II. Fig. 1 displays the numerical complexity of MREC relative to that of MRC, for $L=5$, $T=11$, and $K=42$ (these particular choices are explained later). Note from the upper subplot that BF ($\text{MREC}_{N=1}$) is about 3.4 times less complex than MRC, whereas full MREC is about 1.5 times more complex than MRC. $\text{MREC}_{N=3,4}$ has complexity similar to MRC.

TABLE II
NUMERICAL COMPLEXITY (NO. OF COMPLEX MULTIPLICATIONS/ADDITIONS) FOR L BRANCHES.

Interpolation method	MRC	order-N MREC
SINC	$L(T+1)$	$N(L+T+1)+4LN/K$
MMSE	$L(LT+1)$	$N(L+T+1)+4LN/K$

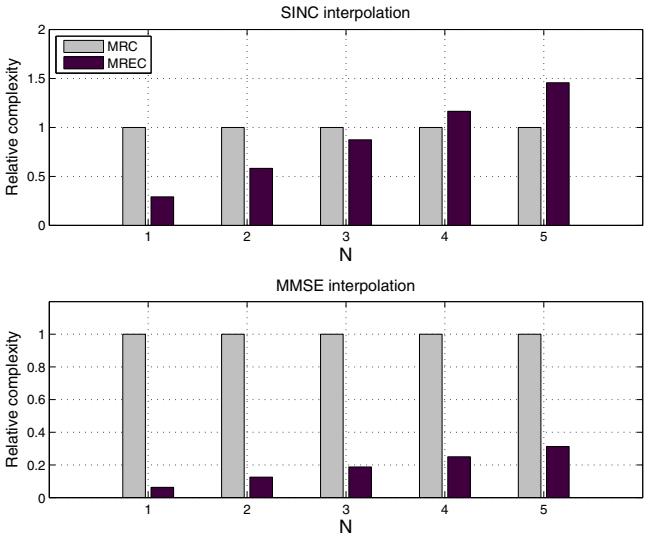

Fig. 1. Numerical complexity of $\text{MREC}_{N=1:L}$ relative to that of MRC, for $L=5$ antenna elements, interpolator length $T=11$, and eigenstructure update period $K=42$ symbols. **Top/Bottom**: SINC/MMSE PSAM.

MMSE PSAM has low-complexity for the estimation of the eigengains (because they are uncorrelated, and thus can be estimated separately) for MREC, but very high complexity for the estimation of the channel gains (because joint estimation is required for vectors with correlated components [4, Section 3.6.2, p. 84]) for MRC. The overall MRC and MREC complexities for MMSE PSAM fading estimation appear in Table II. Fig. 1 displays in the lower subplot the numerical complexity of MREC relative to that of MRC for MMSE PSAM. Note that MRC is 16 times more complex than BF and about 3.2 times more complex even than full MREC. The huge complexity of MRC is due to MMSE PSAM estimation.

D. Optimum Order Selection for MREC

The above discussion suggests that standalone BF or MRC may lead to poor performance or high complexity. Adaptive MREC is proposed as a more efficient solution [5]. The following simple criterion for MREC adaptation was found effective in previous analyses assuming perfectly known eigenstructure [8] [5, Section VI.A]:

$$\min_{N=1:L} E\left\{E_s\cdot\|\mathbf{\Pi}_{L-N}\widetilde{\mathbf{h}}\|^2+\|\mathbf{\Pi}_N\widetilde{\mathbf{n}}\|^2\right\}, \tag{11}$$

where $\|\cdot\|$ stands for Euclidian norm, $\mathbf{\Pi}_N \stackrel{\triangle}{=} \mathbf{E}_N\mathbf{E}_N^H$ is the orthogonal projection on the subspace spanned by the columns

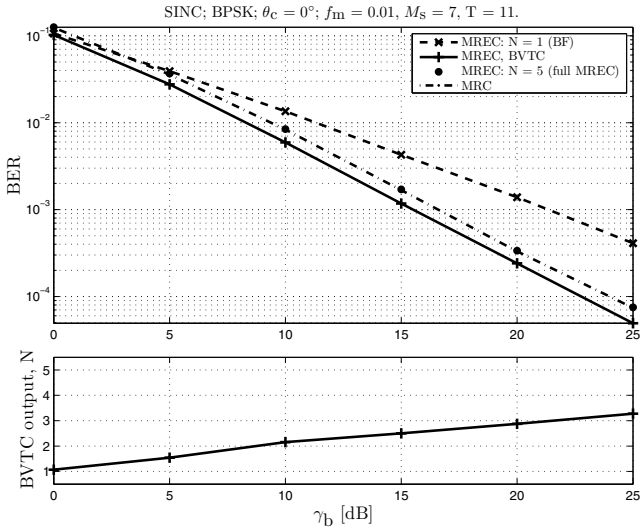

Fig. 2. **Top**: average error rate vs. bit-SNR, for MRC, BF, full MREC and BVTC MREC for SINC PSAM. **Bottom**: MREC order output by the BVTC in average over the AS samples.

of $\mathbf{E}_N$, and $\mathbf{\Pi}_{L-N} \stackrel{\triangle}{=} \mathbf{I}_L - \mathbf{\Pi}_N$. This criterion is equivalent to

$$\min_{N=1:L}\left[E_s\cdot\sum_{i=N+1}^{L}\lambda_i+N_0\cdot N\right], \tag{12}$$

and is better known as the *bias-variance tradeoff* criterion (BVTC) because (12) balances the loss incurred by removing the weakest $(L-N)$ intended-signal contributions (the first term) against the residual-noise contribution (the second term).

IV. SIMULATION RESULTS

A. Independent Log-Normal AS Samples

The simulation results shown in Figs. 2 and 3 were obtained for SINC and MMSE PSAM, respectively, and the following settings: BPSK transmitted signal, receive uniform linear array (ULA) with $L=5$ and $d_n=1$, normalized Doppler shift $f_m=0.01$ (i.e., mobile station with velocity $v=60$ km/h transmitting at rate $f_s=10$ kbps on a carrier with frequency $f_c=1.8$ GHz), slot length $M_s=7$, interpolator length $T=11$, and approximate combining. At each value of the bit-SNR γ_b — defined to include the pilot symbol energy (equal to that of the data symbol), as in [4, Eqn. (2.84), p. 38] — the same 30 independent AS samples from the log-normal distribution from (5) were considered. For each AS sample the first 120 slots were used for training (i.e., initial channel fading and eigenstructure estimation), and then the data symbols of 25000 slots were detected. The channel eigenstructure was updated with the PASTd algorithm, taking one received signal vector sample every 6 slots apart (i.e., $K=42$) in order to ensure low fading correlation between the samples [4, Fig. 2.4, p. 24]. The upper subplots in Figs. 2 and 3 show the average (over noise, fading, and AS) error rates for MRC, BF, full MREC, and BVTC MREC. The lower subplots show the MREC order output by the BVTC in average over the AS samples.

Note that when the fading is estimated using SINC PSAM (i.e., independently of the channel) only the eigenvectors are

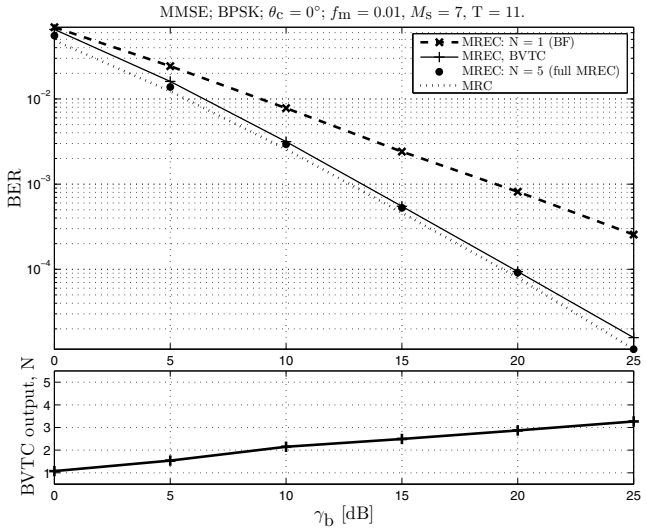

Fig. 3. **Top**: average error rate vs. bit-SNR, for MRC, BF, full MREC and BVTC MREC for MMSE PSAM. **Bottom**: MREC order output by the BVTC in average over the AS samples.

required for the actual implementation of MREC. The eigenvalues are not required. Then, Fig. 2 indicates that PASTd-based full-MREC is nearly performance-equivalent with MRC. Recall from Section III-B3 that full-MREC that employs the true eigenvectors is indeed performance-equivalent with MRC for SINC PSAM. Thus, beside its low complexity, the PASTd algorithm can accurately estimate the channel eigenvectors even for realistic, small-to-moderate AS [5, Fig. 1], which can yield wide eigenvalue spreads for $\mathbf{R}_{\tilde{\mathbf{h}}}$, i.e., ill-conditioned eigendecomposition problem.

Fig. 2 shows that BVTC MREC can significantly outperform BF. For example, at an error rate of 10^{-3} MREC with average order output by the BVTC of 2.5 outperforms BF by more than 6 dB, due to diversity gain, for a 2.5 times higher complexity — see Table II. Interestingly, BVTC MREC even outperforms MRC by about 1 dB, due to suboptimal estimation, approximate combining, and because fewer channel estimation errors are compounded. Finally, BVTC MREC yields a 25% complexity reduction vs. MRC. The complexity-reduction advantage reduces slowly with increasing bit-SNR.

For MMSE PSAM, MRC is performance-equivalent with full-MREC given the true channel eigenstructure. However, for MMSE PSAM, MREC actually uses knowledge of both the eigenvectors and the eigenvalues of $\mathbf{R}_{\tilde{\mathbf{h}}}$, unlike for SINC PSAM. Fig. 3 indicates that, because of the small PASTd eigenvalue estimation error, MRC slightly outperforms PASTd-based full-MREC for MMSE PSAM. Nevertheless, MRC is then 3.2 times more complex than full-MREC. BVTC-based adaptivity can further lower MREC complexity, while preserving near-optimum performance. For example, at error rate of $3 \cdot 10^{-3}$, BVTC MREC (with average order of about 2) underperforms MRC by only about 0.5 dB, for about 8 times lower complexity. On the other hand, BVTC MREC outperforms BF by about 4 dB for 2 times higher complexity. The diversity gain achievable with BVTC MREC over BF increases quickly with lower error rates. Increasing the SNR does not increase the BVTC output (and thus the MREC complexity) as rapidly. MMSE PSAM also outperforms SINC PSAM for all the combining methods.

B. Time-Correlated Log-Normal AS Samples

The simulation results shown in Figs. 4 and 5 were obtained for SINC and MMSE PSAM, respectively, and for the same transmitted signal, fading conditions, antenna geometry, and channel fading and eigenstructure estimation settings as above. The bit-SNR was set to 5 dB. For the typical urban (TU) scenario discussed in Section II-B, the log-normally distributed AS has distance (time) correlation described by (6). A single AS sequence was generated, one sample for every 6 slots (not for every symbol, since the AS would not vary significantly, and $\mathbf{R}_{\tilde{\mathbf{h}}}$ computation using [6, Eqn. 16] [4, Eqns. (4.3)-(4.4), pp. 136-137] would then significantly increase simulation time). The transmission of 90600 slots (of which the first 600 were for used for training) was simulated, i.e., $90600 \times M_S/f_S = 63.42$ s, or $63.42 \times v = 1057\,\mathrm{m} \approx 15\,d_{AS}$. The top subplot in Figs. 4 and 5 displays the AS sequence made of $90600/6 = 15100$ samples. The average error rates shown in the middle subplots for MRC, BF, full MREC, and BVTC MREC were obtained as follows. The 90600 slots were divided into adjacent segments of 600 slots. Note that the AS decorrelation distance, $d_{AS} = 70$ m comprises 10 such segments, which implies relatively constant AS over this BER calculation interval. Moreover, 600 slots provide 100 uncorrelated channel fading samples, which is sufficient for accurate PASTd-based eigenstructure updating. There were 20 runs with the same AS sequence but different channel and noise samples. Thus, the error rates shown in these figures were obtained by averaging over $20 \times 600 \times (M_S - 1) = 72000$ channel and noise samples. The output of the BVTC, i.e., the order for BVTC MREC, appears in the bottom subplots.

Fig. 4 confirms that, for SINC PSAM, full MREC yields near-MRC performance, and demonstrates the ability of BVTC MREC to adapt to the channel AS fluctuations for near-optimum performance at low complexity. Note that for low AS, BVTC MREC and BF can significantly outperform MRC, due to a lower number of estimated fading parameters and a higher effective SNR for the estimation.

Fig. 5 confirms for MMSE PSAM the ability of BVTC MREC to adapt to the channel AS fluctuations and thus reap great performance benefits compared to BF as well as significant complexity reductions compared MRC. Note however that for MMSE PSAM estimation MREC does not underperform MRC at low AS.

Note that the above numerical results obtained by simulation follow closely the numerical results obtained from analysis in previous work [4] [5] demonstrating the good subspace-tracking performance of the low-complexity PASTd algorithm.

V. Summary and Conclusions

The paper has presented performance and complexity comparisons between traditional smart antenna algorithms,

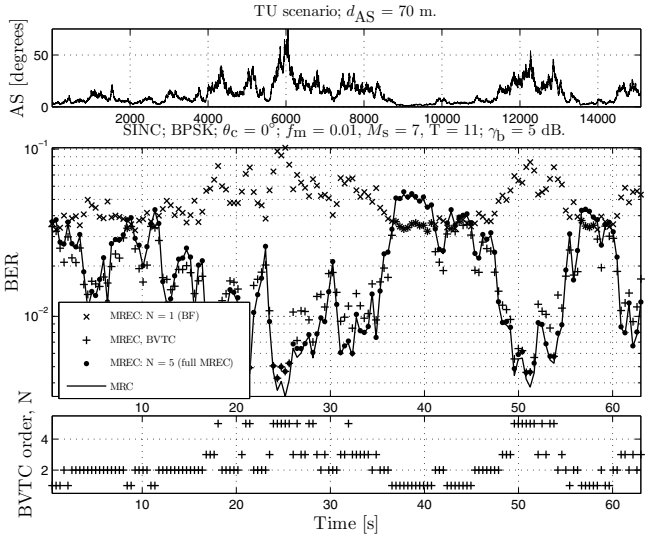

Fig. 4. **Top**:15,000 lognormal correlated AS Samples for a TU scenario. **Middle**: Average symbol error rate for BPSK for BF, MRC, and MREC adapted with BVTC and $L = 5$ full MREC, and SINC interpolation with $T = 11$. **Bottom**: MREC order selected with the BVTC.

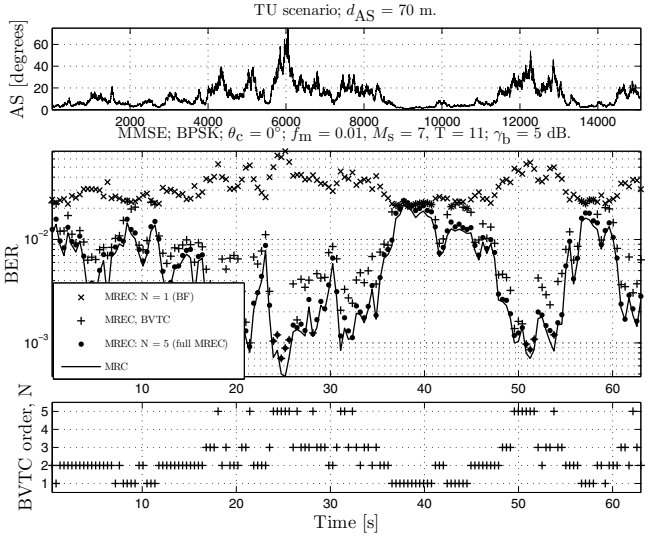

Fig. 5. **Top**:15,000 lognormal correlated AS Samples for a TU scenario. **Middle**: Average symbol error rate for BPSK for BF, MRC, and MREC adapted with BVTC and $L = 5$ full MREC, and MMSE interpolation with $T = 11$. **Bottom**: MREC order selected with the BVTC.

i.e., statistical beamforming (BF) and maximal-ratio combining (MRC), and their recently-proposed superset known as maximal-ratio eigencombining (MREC). The appeal of eigencombining lies in its ability to adapt to the actual channel fading spatial correlation, which in practice varies due to slow fluctuations in azimuth spread (AS). We have found that Yang's low-complexity deflation-based projection approximation subspace tracking (PASTd) algorithm updates accurately the channel eigenstructure required for MREC adapted to the actual AS with the bias-variance tradeoff criterion (BVTC). Simulations that agree with previous analysis results indicate that, for suboptimal channel fading estimation, a uniform linear array with 5 antenna elements employing BVTC-based adaptive MREC can outperform MRC by about 1 dB for half of the computation requirements of MRC. Interestingly, at an error rate of 10^{-3}, BVTC MREC outperforms the half-as-complex BF by more than 6 dB, because of diversity gain. For optimal channel fading estimation and error rate $3 \cdot 10^{-3}$, BVTC MREC underperforms MRC by only about 0.5 dB, but offers about 8 times lower complexity. On the other hand, BVTC MREC outperforms BF by about 4 dB for double the BF computational complexity. Our results demonstrate the great ability of PASTd-based BVTC MREC to adapt to AS fluctuations. Future work will focus on employing MREC for more realistic channel models in which the AS actually affects the fading distribution type.

REFERENCES

[1] A. Hottinen, M. Kuusela, K. Hugl, J. Zhang, and B. Raghothaman, "Industrial embrace of smart antennas and MIMO," *IEEE Wireless Communications*, vol. 13, no. 4, pp. 8–16, August 2006.

[2] A. Paulraj, R. Nabar, and D. Gore, *Introduction to Space-Time Wireless Communications*. Cambridge, UK: Cambridge University Press, 2005.

[3] A. Algans, K. I. Pedersen, and P. E. Mogensen, "Experimental analysis of the joint statistical properties of azimuth spread, delay spread, and shadow fading," *IEEE Journal on Selected Areas in Communications*, vol. 20, no. 3, pp. 523–531, April 2002.

[4] C. Siriteanu, "Maximal-ratio eigen-combining for smarter antenna array wireless communication receivers," Ph.D. dissertation, Queen's University, Kingston, Canada, 2006.

[5] C. Siriteanu and S. D. Blostein, "Maximal-ratio eigen-combining for smarter antenna arrays," *IEEE Transactions on Wireless Communications*, vol. 6, no. 3, pp. 917 – 925, March 2007.

[6] C. Sun, J. Cheng, and T. Ohira, Eds., *Handbook on Advancements in Smart Antenna Technologies for Wireless Networks. Chapter 'Eigencombining: A Unified Approach to Antenna Array Signal Processing' by C. Siriteanu et al.* New York, NY: Idea Group, Inc., 2008.

[7] C. Brunner, W. Utschick, and J. A. Nossek, "Exploiting the short-term and long-term channel properties in space and time: eigenbeamforming concepts for the BS in WCDMA," *European Transactions on Telecommunications. Special Issue on Smart Antennas*, vol. 12, no. 5, pp. 365–378, 2001.

[8] C. Siriteanu, S. D. Blostein, and J. Millar, "FPGA-based communications receivers for smart antenna array embedded systems," *EURASIP Journal on Embedded Systems. Special Issue on Field-Programmable Gate Arrays in Embedded Systems*, vol. 2006, pp. Article ID 81 309, 13 pages, 2006.

[9] M.-S. Alouini, A. Scaglione, and G. B. Giannakis, "PCC: principal components combining for dense correlated multipath fading environments," in *Proc. IEEE Vehicular Technology Conference, (VTC '00)*, vol. 5, September 2000, pp. 2510–2517.

[10] F. A. Dietrich and W. Utschick, "Maximum ratio combining of correlated Rayleigh fading channels with imperfectly known channel," *IEEE Communications Letters*, vol. 7, no. 9, pp. 419–421, September 2003.

[11] B. Yang, "Projection approximation subspace tracking," *IEEE Transactions on Signal Processing*, vol. 43, no. 1, pp. 95 – 107, January 1995.

[12] W. Utschick, "Tracking of signal subspace projectors," *IEEE Transactions On Signal Processing*, vol. 4, no. 50, pp. 769 – 778, April 2002.

[13] 3GPP, "Technical Specification Group Radio Access Network. Spatial Channel Model for Multiple Input Multiple Output (MIMO) Simulations, Release 6," 3rd Generation Partnership Project (3GPP), Tech. Rep. TS 25.996, 2003.

[14] M. K. Simon and M.-S. Alouini, *Digital Communication over Fading Channels. A Unified Approach to Performance Analysis*. Baltimore, Maryland: John Wiley and Sons, 2000.

[15] C. Siriteanu and S. D. Blostein, "Maximal-ratio eigencombining: a performance analysis," *Canadian Journal of Electrical and Computer Engineering*, vol. 29, no. 1/2, pp. 15–22, January–April 2004.